Joint Migration Inversion of 3D Full Wavefield Borehole Data

El Marhfoul, Bouchaib; Verschuur, D.J.

Publication date
2017

Document Version
Final published version

Published in
Proceedings of the 79th EAGE Conference & Exhibition 2017, Paris, France, 12-15 June 2017

Citation (APA)
El Marhfoul, B., & Verschuur, D. J. (2017). Joint Migration Inversion of 3D Full Wavefield Borehole Data. In *Proceedings of the 79th EAGE Conference & Exhibition 2017, Paris, France, 12-15 June 2017* EAGE.

We P9 06

Joint Migration Inversion of 3D Full Wavefield Borehole Data

B. El Marhfoul* (Delft University of Technology), D.J. Verschuur (Delft University of Technology)

Summary

3D borehole-related seismic data can provide us with accurate velocity models and high-resolution images. However, conventional imaging algorithms that assume primary reflection energy will cover only a limited area around the borehole. This illumination problem can be overcome by including surface-related and internal multiples in the imaging algorithm to enhance the illumination of the subsurface and image areas that are beyond the coverage of primary reflections. The industry standard for 3D borehole imaging is to use the first breaks to update the velocity model and consider only the primary reflections for imaging. It has been demonstrated that multiple scattering and the down-going wavefield can tremendously extend the imaging area around the borehole. Moreover, primary and multiple scattering contain valuable and crucial information that can enable us to update the velocity model beyond the coverage area of the first arrivals.

In this paper we have employed the full wavefield of the 3D borehole data - containing all order scattering in both up/ down-going wavefields - in one integrated inversion-imaging process as proposed by the joint migration inversion methodology. The final result is a smooth accurate background velocity model along with a true amplitude reflectivity high-resolution image with and maximum lateral extent.

Introduction

In the case of datasets with sparse acquisition geometry, like 3D borehole-related seismic data, conventional imaging algorithms produce images with limited lateral extent (Blias and Hughes, 2015). Furthermore, given the poor fold distribution, no adequate update of the velocity model can be performed. The multiple scattering and the down-going wavefield are valuable signals present in the seismic data (Lee and Gou, 2016). They provide us with huge opportunities and virtues to enhance both the reflectivity image and its corresponding background velocity model on the condition that the right inversion-imaging algorithm is used (Berkhout, 2014b). Using forward modeling of the measured data based on reflectivity and propagation operators via full wavefield modeling (FWMod, Berkhout, 2014a), it is possible to derive an inversion process called JMI (Joint Migration Inversion) (Berkhout, 2014b). With JMI the involved inversion problem becomes less non-linear by decoupling propagation operators that describe the kinematics from the scattering operators that affect the amplitude in the seismic data. JMI applied to 3D VSP data is an extension of the full wavefield migration (FWM) algorithm for VSP data (Soni and Verschuur, 2014; El-Marhfoul and Verschuur, 2014) by including and allowing the update of the 3D velocity model. It is an iterative process, where the modeled data is constructed in a recursive manner and continuously compared with the measured input data. The residue is then translated into an update of the reflectivity and the velocity model in a flip-flop manner. All multiples – surface and internal – are considered as part of the illuminating wavefield and a full waveform inversion approach is used to find reflectivity and propagation operators such that the measured data via FWMod is fully explained. In this way multiples do not wrongly map in the image, but will contribute in the illumination of areas not well covered by primaries.

The output of the JMI algorithm is a smooth background velocity and a high-resolution reflectivity model that explain the propagation effects and all order scattering energy. Staal (2014) has already successfully demonstrated the JMI concept on 2D surface seismic data and El-Marhfoul and Verschuur (2016) for the 3D case. The significant contribution of multiple scattering and the down-going wavefield to the imaging was successfully demonstrated by El-Marhfoul and Verschuur (2015). In this paper, the JMI algorithm is demonstrated on the full wavefield of 3D borehole data including the down-going wavefield such that the expected value of acquiring 3D VSP data (see e.g. Gerea et al., 2016) will be even more increased.

Joint migration inversion of 3D VSP data

With the recently developed paradigm of JMI, as explained by Berkhout (2014b), it is possible to simultaneously invert the full wavefield of the 3D borehole data including the down-going wavefield. In the end, the same earth should explain all types of measurements. It will automatically mean that energy from the multiple scattering and the down-going wavefield will be focused into the right position and, hence, will extend the lateral coverage of the image. Moreover, the extra sensitivity of the multiples to erroneous propagation operators puts additional constrains on the possible solutions for the velocity model and will help expediting and steering inversion algorithms toward more reliable estimates.

By using reciprocity and exchanging the sources and receivers positions in the 3D VSP data, 3D shot records are obtained, similar to surface seismic data, with the receivers depth as sources elevation. In the frequency domain every ‘shot’ record number j ‘measured’ at all surface locations is then written as vector $\vec{P}_j^-(z_0, z_{src})$. Within the framework of JMI, the modeled data is continuously compared to the measured data, after having updated the reflectivity and velocity model. By closing the loop in the inversion-imaging process and feeding back the residual data to the JMI engine, optimized reflectivity and velocity models will be obtained. Therefore, the following cost-function will be minimized, based on a conjugate gradient scheme, to obtain a smooth background velocity model and a true amplitude reflectivity image:

$$J = \sum_{j} \sum_{\omega} \left\| \vec{P}_j^-(z_0, z_{src}) - \sum_{m} \mathbf{W}^-(z_0, z_m)\delta\vec{S}_j(z_m, z_{src}) \right\|, \tag{1}$$

with the scattered wavefield at each depth level z_m defined as

$$\delta\vec{S}_j(z_m, z_{src}) = \mathbf{R}^{\cup}(z_m)\vec{P}_j^+(z_m, z_{src}) + \mathbf{R}^{\cap}(z_m)\vec{P}_j^-(z_m, z_{src}), \tag{2}$$

where $\vec{P}_j^+(z_m, z_{src})$ and $\vec{P}_j^-(z_m, z_{src})$ are the incident wavefields reaching depth level z_m from above and below, respectively, from shot number j. $\mathbf{R}^{È}(z_m)$ and $\mathbf{R}^{Ç}(z_m)$ are the angle dependent reflectivity matrix from above and below. $\mathbf{W}^-(z_0, z_m)$ brings the reflected wavefield from depth level z_m to the surface, where all reflection energy is observed as $\vec{P}_j^-(z_0, z_{src})$ for 'shot' number j at elevation z_{src}. Note that we used the relation for transmission $\mathbf{T}^+(z_m) = \mathbf{I} + \mathbf{R}^{\cup}(z_m)$, which is only strictly valid for acoustic media. In the JMI approach, the incident wavefields at depth level z_m are recursively built from the original down-going source fields and the coda of multiples generated by the imaged reflectivities. Thus, the final image is reliable, laterally consistent with all types of measurements and will inherit the resolution of the data that is measured close to the reflection points.

3D Numerical example

In this section we will illustrate the 3D JMI for a relatively small 3D subsurface model that is selected from the 3D SEG salt model. In Figure 1, we see a display of the 3D velocity model along with the true reflectivity model, which is derived from it. The model covers a total area of 6 Km by 6 Km and a total depth of 2 Km. 3D VSP seismic data was modeled, with a maximum frequency of 20 Hz, using reciprocity meaning that for the modeling and the imaging process the sources are assumed in the well, while the receivers were located at the surface. The well location was set close to the fault at the cross-section in Figure 1. The 3D VSP data was modeled, for thirty-seven levels with elevation starting from z = 0 m up to z = 1440 m with Δz = 40 m. The receiver grid is fixed and is densely sampled over the complete areal extent of the model according to a uniform grid with Δx =Δy = 20 m.

In this numerical example, we have started the JMI process with a 1D velocity, as depicted in Figure 2. In Figure 3, we see the results of the JMI algorithm for the estimated velocity and reflectivity model, where the full wavefield (primaries, multiples and down-going wavefield) is deployed in the inversion process. In spite of the sparse acquisition geometry, at the borehole side, the 3D JMI algorithm was able to update the velocity model and steer it toward a reasonable solution. This is mainly because the multiple scattering and the down-going wavefield are reinforcing the primary energy during the inversion process. It can clearly be noticed that the JMI algorithm has succeeded in updating the velocity model even in areas beyond the coverage of primary reflections, which is due to the contribution of the multiple scattering and the down-going wavefield. Furthermore, the main features of the salt structure are retrieved, despite the poor quality of the starting model. The obtained velocity model has a smooth profile that explains the kinematics in the seismic data and the high-resolution details can be found in the corresponding reflectivity model. Note the tremendous improvements in the final image compared to the estimate from the first iteration, which is equivalent to the output of conventional PSDM. The final estimate of the reflectivity is consistent with the true reflectivity model, within the area that is adequately illuminated by the total wavefield, and has maximum lateral coverage with a resolution that is determined by the seismic data frequency bandwidth. Figure 4 shows a lateral cross-section from the final 3D JMI reflectivity model. The contribution of the multiple scattering and the down-going wavefield is clearly noticeable. The shallow part of the image has a large lateral extent and the salt body is better illuminated, even beyond areas outside the coverage range of primary reflections. Furthermore, the high angles present in the 3D borehole data make the JMI algorithm more sensitive to erroneous velocities, hence, expediting and steering the algorithm to a more accurate solution.

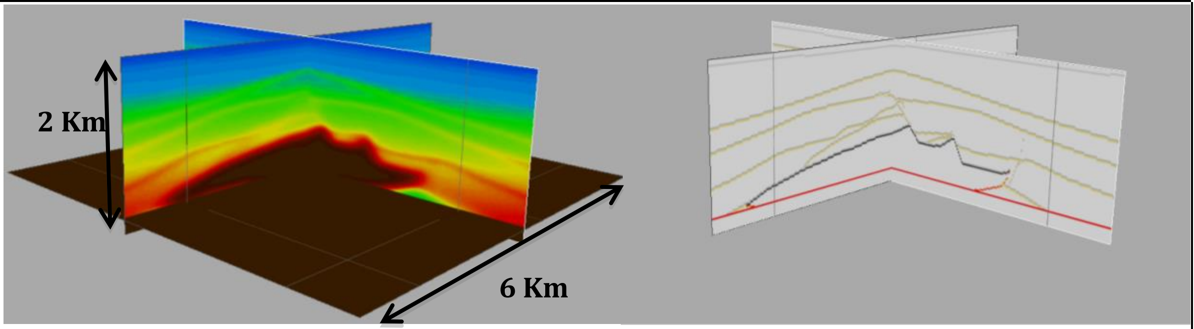

Figure 1: The true velocity model and its corresponding reflectivity. The well is located at the cross-section of the two planes, where VSP data are obtained from 0 – 1440 m depth.

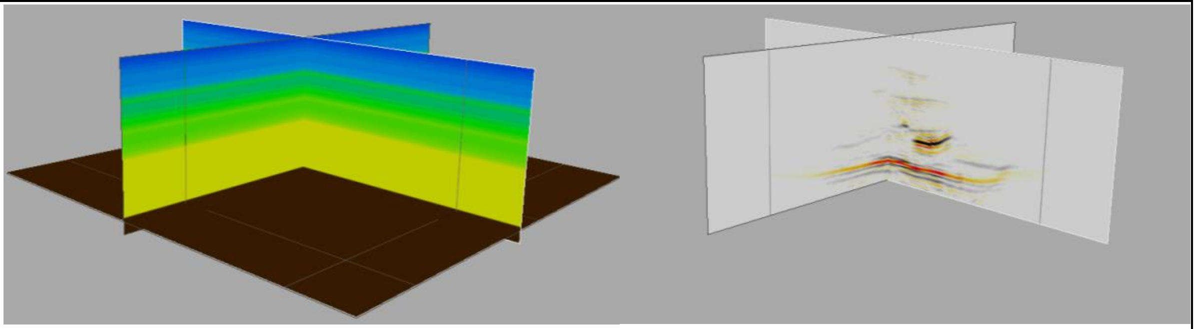

Figure 2: The starting velocity model and the 3D reflectivity estimate from the first iteration, which is equivalent to conventional imaging (PSDM).

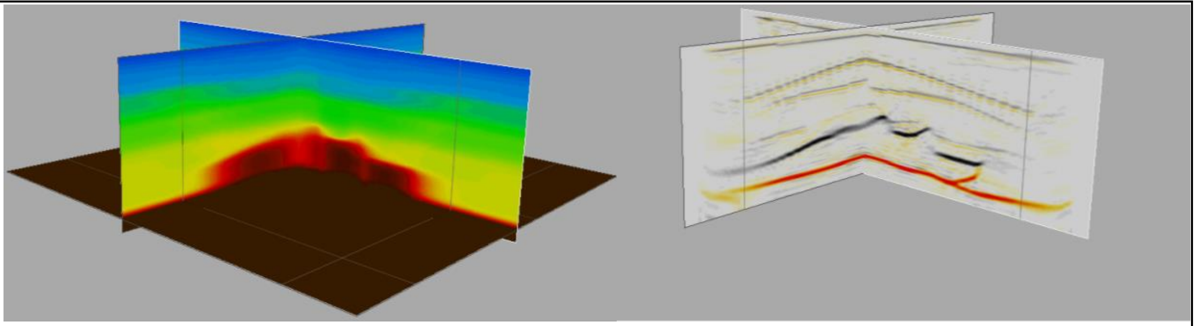

Figure 3: The 3D JMI final model and its corresponding reflectivity model. Note the maximum lateral extent in both velocity and refelctivity, mailny due to the multiples.

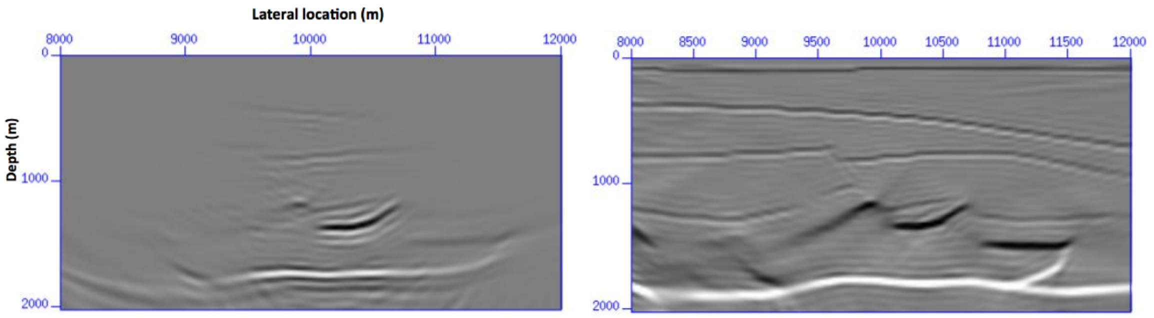

Figure 4: Lateral cross-section from the 3D JMI refelctivity (right handside image) compared with PSDM image (left handside image). Note the better focusing and the right positioning of the salt body.

Conclusions

In this paper, the JMI algorithm is applied to the full wavefield (primaries, multiples and down-going wavefield) of 3D borehole data. By using reciprocity and exchanging the sources and receivers positions in the 3D VSP data, 3D buried-shot records are obtained, with the receivers depth at sources elevation and the source at the receiver depth. Within JMI, the modeled data is continuously compared to the measured data, after having updated the reflectivity and the velocity model. By closing the loop in the inversion-imaging process and feeding back the residual data to the JMI engine, an optimized reflectivity and velocity model will be obtained. In spite of the sparse acquisition geometry, the 3D JMI algorithm was able to provide good estimate of the velocity and reflectivity model, mainly because of the high angles available in the VSP data and the contribution from the multiple scattering and the down-going wavefield. The numerical example presented in this paper shows the effectiveness of the JMI approach, even in a complex environment, in retrieving the right kinematics properties from 3D borehole data and translate it into proper velocity update.

Acknowledgements

The authors thank the sponsoring companies of the Delphi research consortium for their support.

References

Berkhout, A. J., 2014a, Review Paper: An outlook on the future of seismic imaging, Part I: Forward and reverse modelling: Geoph.Prosp., **62**, 911–930.

Berkhout, A. J., 2014b, Review Paper: An outlook on the future of seismic imaging, Part III: Joint Migration Inversion: Geoph.Prosp., **62**, 950–971.

Blias, E. and B. Highes, 2015, 3D VSP imaging: general problems: 85th Ann. Internat. Mtg., Soc. Expl. Geophys., Expanded abstracts, 5630-5635.

El-Marhfoul, B., and D.J. Verschuur, 2014, 3D Joint Full Wavefield Imaging of Surface and VSP Data: 84th Ann. Internat. Mtg., Soc. Expl. Geophys., Expanded abstracts, 5070-5074.

El-Marhfoul, B., and D.J. Verschuur, 2015, 3D Full Wavefield Imaging of Up and Down-Going VSP Data: 77th Ann. Internat. Mtg., Eur. Ass. of Geosc. and Eng., Expanded abstracts.

El-Marhfoul, B., and D.J. Verschuur, 2016, High-resolution, integrated 3D Joint Migration Inversion of Surface and VSP Data: 78th Ann. Internat. Mtg., Eur. Ass. of Geosc. and Eng., Expanded abstracts.

Gerea, C., P.L. Pichon, G. Geddes, M. Verliac and V. Lesnikov, 2016, Proficient subsalt monitoring with 3D well seismic, deep-offshore West Africa: 86th Ann. Internat. Mtg., Soc. Expl. Geophys., Expanded abstracts, 688-692.

Lee, C.C. and W. Gou, 2016, 3D VSP processing and imaging: a case study at Mad Dog, Gulf of Mexico: 86th Ann. Internat. Mtg., Soc. Expl. Geophys., Expanded abstracts, 5562-5566.

Soni, A. K. and D.J. Verschuur, 2014, Full-wavefield migration of vertical seismic profiling data: using all multiples to extend the illumination area: Geoph.Prosp., **62**, 740-759.

Staal, X.R. , D.J. Verschuur and A.J. Berkhout, 2014, Robust Velocity Estimation by Joint Migration Inversion: 76th Ann. Internat. Mtg., Eur. Ass. of Geosc. and Eng., Expanded abstracts, 4290-4295.